# Regional Conditions During The 25 October 1986 FIRE Cirrus/Altocumulus Case Study

David O'C. Starr
NASA Goddard Space Flight Center
Greenbelt, MD 20771

Kenneth Sassen
Department of Meteorology
University of Utah
Salt Lake City, UT 84112

The regional cloud and meteorological conditions are described for this case using satellite imagery (GOES), dual polarization lidar data (from Wausau), NWS radar, NMC analyses, rawinsonde data including special soundings, and analyzed vertical motions. These observations are interpreted with respect to relationships between the observed cloud characteristics and corresponding atmospheric structure. Similarities with the 27-28 October FIRE Cirrus Case Study are noted.

Visible satellite imagery reveals overcast conditions over the upper Midwest at 2000 UTC on 25 October (Fig. 1a). Radar observations showed a band of light precipitation across southeastern Wisconsin at that time (echo tops to 7 km). Drizzle and light rain were also found to the south where the clouds were brightest. The decreased cloud albedo over southern Wisconsin indicates the presence of overlying cirrus clouds. The cirrus are more evident in the infrared imagery where a band of cold clouds stretches from western Iowa to Michigan (Fig. 1b). To the north and south of this feature, the high clouds appear more variable and were responsible for the patches of lower albedo seen over northern Illinois (Fig. 1a).

These clouds were associated with a nearly stationary occluded cyclone at the surface and closed low aloft (Fig. 2). The cyclone was centered in southern Illinois with the occluded front lying through southern Indiana and then southward to Georgia. The high clouds were located in the exit region of the upper level vortex and were bounded on the west by the interface between northerly flow (entrance) and southerly flow (exit). The northern boundary of the cirrus (Fig. 1b) lay along the transition between southerly flow out of the closed low and westerly flow in Canada. The cloud features moved steadily to the NNW during the afternoon.

Surface-based, dual-polarization lidar observations at Wausau prior to 1730 UTC detected fairly dense midlevel cirrostratus between 5.5 and 8 km (Fig. 3a). Observed polarization ratios ($\delta$) of 0.55 to 0.65, corresponding to rimed (or very complex) ice crystals, were widespread in the lower portion of the cloud (Fig. 3b). At about 1730 UTC, cloud base height began to increase rapidly and evidence of supercooled liquid water was found between 7.8 and 8 km ($\delta \leq 0.15$). An overlying layer of cirrus between 9.5 and 11.1 km was observed at this time. Concurrent satellite observations indicate that this higher cirrus layer was present earlier but obscured by the midlevel cloud. Lidar observations after 1900 UTC may have also been significantly attenuated by the midlevel cloud layer. Subtropopause cirrus were sporadically detected above 10.5 km and another cirrus layer was observed between 8.5 and 9.8 km around 2000 UTC (Fig. 3a). Airborne observers noted the distinct clear region between this cirrostratus layer and the underlying midlevel cloud (Shanot, personal communication).

From 1900 to 2030 UTC during the King Air flight operations near Wausau, altocumulus clouds were observed between 7.8 and 8.1 km (-31 to -33 C) capping a 2.5-km deep ice cloud with a variable base around 5.5 km. Values of $\delta$ in the ice cloud were generally near 0.3 which is characteristic of some forms of cirrus. Low depolarization ratios ($\delta \leq 0.15$) in the ice cloud were likely associated with oriented plate crystals in sheared fallstreaks (in contrast to the liquid phase altocumulus layer, significantly increased $\delta$ and decreased return energy were found when the lidar was tipped off vertical by a few degrees - points labelled "x" along the bottom of Fig. 3). The strongest orientation effects were apparent below 7 km and well below the base of the altocumulus layer. This indicates that growth of the crystals to sizes greater than 200 mm, as required to maintain a stable orientation, or a change to a less complex crystal habit occurred during sedimentation. The flight crew of the King Air reported a continuous sloping cloud base during transit from Wausau, where cloud base was near 5.5 km, to Madison (2030 UTC), where the base height was about 3 km and drizzle was observed from a lower cloud layer.

Vertical velocities were estimated using the adiabatic method (three-station technique with an estimated uncertainty of $\pm 2$ cm $s^{-1}$) applied to rawinsonde data from eight stations as in Starr and Wylie (1989). The location of the analyzed band of weak ascent (Fig. 4) on the 321 K isentropic surface (7.7 km at Green Bay and 8.2 km at Platteville in southwestern Wisconsin) corresponds very well to the position of the band of cold clouds (cirrus over midlevel cloud, Fig. 1b) at 0000 UTC on the 26th . Ascent rates of more than 3 cm $s^{-1}$ were found at this level.

The corresponding vertical velocity profile computed from soundings at Green Bay (GRB), St. Cloud (STC) and Platteville (PLA) is shown in Fig. 5. The 1800 UTC profile (supplemental soundings at those stations) is consistent with upper level cloud generation at two primary levels - near the tropopause (11 km) where cirrus were detected and near the level where the altocumulus cloud layer was observed. Later, more uniform uplift is indicated throughout the upper troposphere when cirrus cloudiness was detected in the intervening layer (Fig. 3a). The fact that the maximum ascent rate at 1800 UTC was diagnosed above the altocumulus layer is not necessarily inconsistent with the observed cloud location since, as noted by Gedzelman (1988), the pre-existing vertical structure of water vapor plays a major role in determining the level of cloud formation. Rawinsonde-resolved vertical motions were quite weak below the level of the altocumulus layer where the adjoining 2.5-km deep ice cloud was observed.

Rawinsonde data from three soundings that ascended through the cloud band are shown in Fig. 6 - see Starr and Wylie (1989) for discussion of data quality. At Platteville (PLA), ice-supersaturation was observed at all levels colder than 0 C (no data at temperatures colder than -50 C), except for a layer from 8.9 to 9.7 km where relative humidity with respect to ice (RHI) decreased to 95% (Fig. 6a). Relative maxima of 102% were measured from 7.8 to 8.4 km and at the 9.9 km level (-50 C) corresponding to relative humidity with respect to pure liquid water (RH) of 73% and 64%, respectively. Greater humidities were found at lower levels (RHI = 108% at 5.5 km). The Wausau (WAU) sounding (released at 1855 UTC) exhibited more structure with RHI equal to 112% (RH = 85%) from 7.5 to 7.6 km (RHI $\geq$ 100% from 6.8 to 7.8 km) and decreasing to 60% at -50 C and to 67% at -14 C (5.5 km). The lower vertical-resolution (standard) sounding at Green Bay (GRB) showed ice-supersaturation at 5.6 km (105%) and 7.7 km (101%) with drier but still humid conditions between these levels (RHI = 91% and 75% at 6.6 and 7.3 km, respectively) and above (91% and 86% at 8 and 8.9 km, respectively). Thus, each sounding indicates a relative humidity maximum near 7.8 km corresponding to ice-supersaturation but subsaturated with respect to the liquid phase. Both the GRB and PLA soundings show moist conditions at most levels while, except for the layer from 6.8 to 7.8 km, the WAU sounding is significantly drier. On this basis, it appears that the GRB and PLA soundings were representative of the more disturbed conditions to the south of Wausau where the base of the altocumulus-topped, midlevel, ice cloud extended to below 5.5 km.

The temperature profiles each show an inversion-capped boundary layer with a second inversion near the 3 km level at WAU and GRB (Fig. 6a). At WAU, a third inversion was found at 5 km. Tropopause heights ranged from 10.6 km at PLA to 11.2 km at WAU (11 km at GRB). The Platteville sounding is generally colder than the other two at a given height but this is mostly the result of the lower surface pressure (0.4 kPa) at PLA. Static stability structure is more evident in the potential temperature profiles (Fig. 6b). The high vertical-resolution sounding from Wausau exhibits a lot of fine structure in the upper troposphere that is not found in the PLA sounding of comparable resolution.

A striking feature of the GRB sounding is the nearly dry adiabatic stratification found from 6.6 to 7.3 km (9.4 C $km^{-1}$). This layer was capped by a relatively stable layer (5.8 C $km^{-1}$) extending to the 8 km level. There is also evidence for a statically stable layer at both Wausau (6.1 C $km^{-1}$ from 7.7 to 8 km) and Platteville (7 C $km^{-1}$ from 8 to 8.2 km) although the feature was weaker at those locations. The height of the stable layer corresponds closely to that of the thin, supercooled liquid phase, altocumulus layer observed over Wausau.

If the anomalously cold data point at the 7.3 km level in the GRB sounding is removed (regarding it as erroneous - possibly due to evaporative cooling of a wetted thermistor), the stable layer then extends from 7.7 to 8 km in accord with the other two soundings. In this case, the stratification below 7.7 km is also comparable in each of the soundings - lapse rates within 0.5 C $km^{-1}$ of the ice-pseudoadiabatic lapse rate down to the 6.6 km level. The Green Bay sounding is still conditionally unstable in this layer but only slightly. Below 6.6 km, the GRB and PLA soundings become increasingly stable while the lapse rate at Wausau remains close to ice-pseudoadiabatic down to the inversion at the 5 km level. It is also of note that lapse rates were near ice-pseudoadiabatic in the layer where the overlying cirrostratus layer was observed - within 0.3 C $km^{-1}$ from 8.5 to 9.8 km at WAU.

Upper level winds at Platteville were generally stronger than at Green Bay (Fig. 6c), especially from 8 km to the tropopause (unfortunately, the wind observations from Wausau were unusable). Of particular note is the more southerly wind directions found at GRB in the layer where the altocumulus layer and underlying ice cloud were observed (5.5 to 8 km). This may be interpreted as indicating deformation along the cloud band (see Figs. 1b and 2). The computed vertical velocity profile at 1800 UTC (Fig. 5) implies that horizontal mass convergence existed from roughly the 5 km level to near 9 km and was strongest between 7.5 and 8.5 km with divergence from 9 to 10.5 km and convergence from there to the tropopause. [Computed divergence profiles exhibited large variations depending on the stations used - probably attributable to the mesoscale character of the situation as discussed by Starr and Wylie (1989). Corresponding vertical velocity profiles computed by the kinematic method were judged to be relatively useless.] Similarly, convergence is indicated from 6.5 to 8.5 km at 0000 UTC on the 26th with divergence below.

Relatively strong wind shear was observed near the tropopause at both locations as wind direction veered from SE to SSW in the lower stratosphere. Weak veering was found near the 7 km level at PLA in association with a relative minima in wind speed. A similar feature occurred at GRB but at a lower height (near 6 km). Weak backing was found from there to 8.5 km.

In summary, regional analysis of the available rawinsonde data show that the supercooled altocumulus cloud occurred in a statically stable layer (7.8 to 8.1 km). Saturation was likely induced by adiabatic cooling due to weak ascent (~2 cm $s^{-1}$) and enhanced by infrared cooling as described by Gedzelman (1988) and Starr and Cox (1985b) - solar warming was suppressed by the overlying cirrostratus cloud. Cellularity in the cloud was likely induced by infrared cooling at cloud top (see Starr, 1987b). Dynamic interaction with the adjoining 2.5-km deep ice cloud below

may also have been significant given the near ice-pseudoadiabatic stratification observed from 6.6 to 7.7 km which is consistent with weak convective overturning.

Uplift was associated with horizontal mass convergence that was strongest above 7.5 km. Given that the midlevel moisture supply associated with the convergent flow was fed by the more disturbed conditions to the south where precipitation was observed (echo tops to 7 km), the stable layer in which the altocumulus formed would be consistent with maximum detrainment of cloud water at that level in the disturbed region and maintenance of the midlevel cloud layer downstream. Furthermore, downward growth of the underlying ice cloud via ice particle sedimentation would be consistent with horizontal moisture supply near cloud top and maintenance of convective overturning (Starr and Cox, 1985a; Starr and Wylie, 1989) in the absence of significant mean ascent below the 7 km level. Maintenance of convective currents in the ice cloud would provide further moisture to the cloud by recycling vapor from evaporated particles below (Starr and Cox, 1985b).

Some notable similarities to the 27-28 October FIRE Cirrus Case Study (Starr and Wylie, 1989 - conclusions summarized in paper C02.01) are: 1) synoptic control dominated with a persistent cirrus shield maintained over a ridge axis (exit knee in the case here), 2) significant mesoscale structure was evident over a variety of horizontal scales (the long-lived 100 x 500 km altocumulus cloud band and smaller scale [10 km in width] transverse banding in cirrus here, Fig. 1a), 3) cloud generation occurred at multiple levels (optically thin subtropopause cirrus layer, an underlying cirrostratus layer and a lower altocumulus/altostratus/cirrostratus layer), and 4) relatively shallow (< 0.5 km) cloud generation layers were found.

## REFERENCES


Gedzelman, S.D., 1988: In praise of altocumulus. Weatherwise, 41, 143-149.

Starr, D.O'C., and S.K. Cox, 1985a: Cirrus clouds, Part I: A cirrus cloud model. *J. Atmos. Sci.*, **42**, 2663-2681.

_____, 1985b: Cirrus clouds, Part II: Numerical experiments on the formation and maintenance of cirrus. *J. Atmos. Sci.*, **42**, 2682-2694.

_____, 1987b: Effects of radiative processes in thin cirrus. *J. Geophys. Res.*, **92**, 3973-3978.

Starr, D.O'C., and D.P. Wylie, 1989: The 27-28 October 1986 FIRE Cirrus Case Study: Meteorology and Clouds. (accepted by *Mon. Wea. Rev.*).


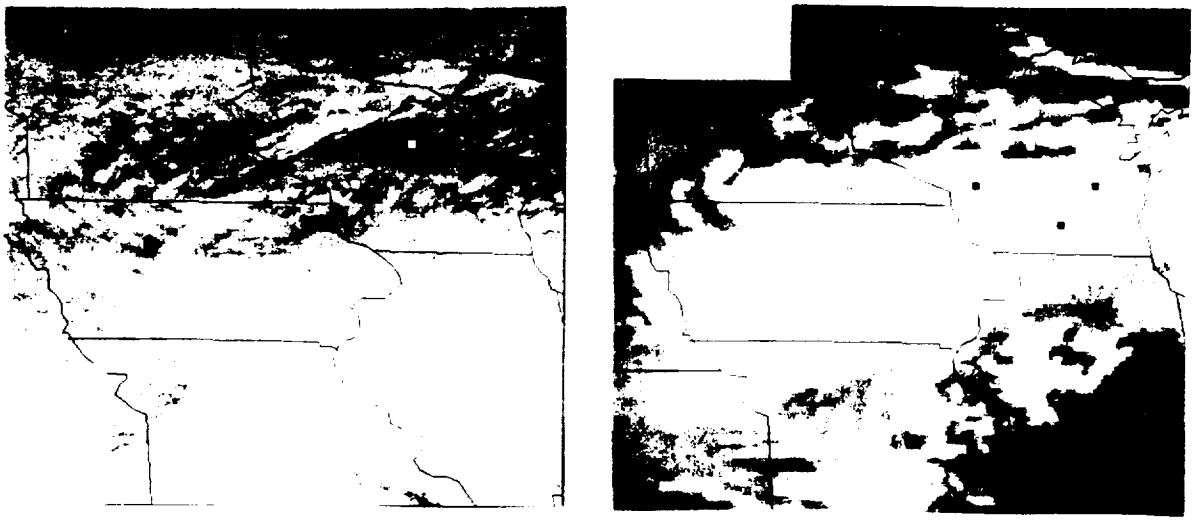

Figure 1: Visible (a) and infrared (b) satellite imagery from GOES-6 at 1800 UTC on 10-25-86.

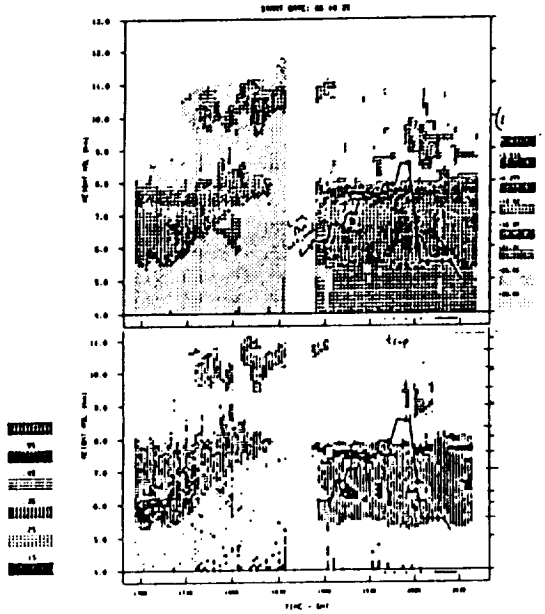

Figure 3: Time-height display of (a) range-corrected returned power (E) and (b) polarization ratio (δ) observed at Wausau by the University of Utah cloud lidar.

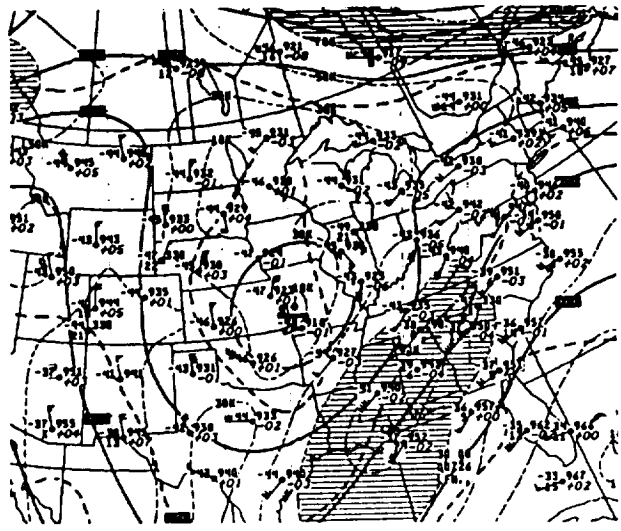

Figure 2: Upper air analyses (30 kPa) at 0000 UTC on 10-26-86.

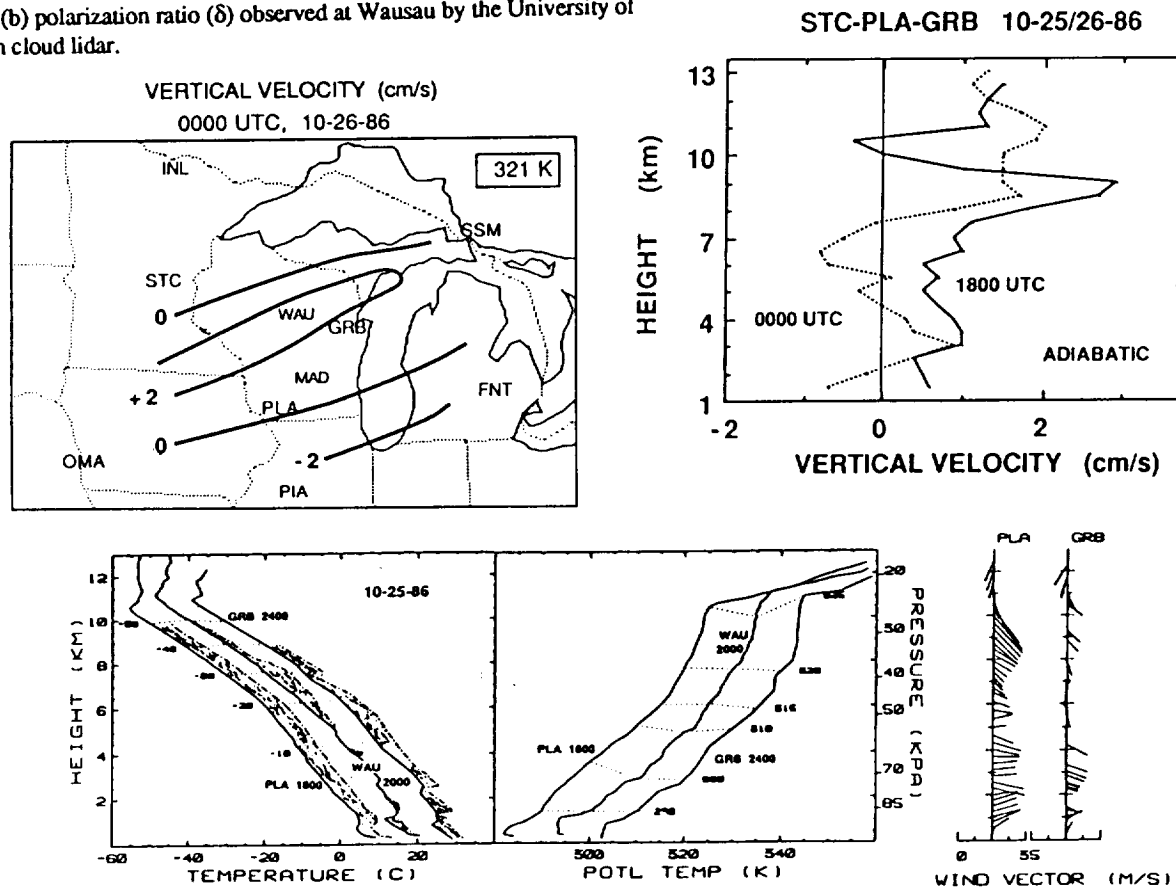


Figure 6: Rawinsonde-observed vertical profiles of a) temperature and relative humidity b) potential temperature, and c) horizontal wind vector observed at Platteville (PLA) at 1800 UTC, Wausau (WAU) at 2000 UTC on 10-25-86 and Green Bay (GRB) at 0000 UTC on 10-26-86. Temperature profiles are plotted on a scale reflecting a 10 C offset with respect to the profile to the left and similarly for potential temperature. Width of the shaded area indicates relative humidity values ranging from 50% to 100% (5°C width) or greater in the case of relative humidity with respect to ice (RHI) which is plotted at temperatures colder than -20 C.